Supersonic Channel Airfoils for Reduced Drag

Stephen M. Ruffin,* Anurag Gupta,[†] and David Marshall[‡]
Georgia Institute of Technology, Atlanta, Georgia 30332-0150

A proof-of-concept study is performed for a supersonic channel-airfoil concept, which can be applied to the leading edges of wings, tails, fins, struts, and other appendages of aircraft, atmospheric entry vehicles, and missiles in supersonic flight. It is designed to be beneficial at conditions in which the leading edge is significantly blunted and the Mach number normal to the leading edge is supersonic. The supersonic channel-airfoil concept is found to result in significantly reduced wave drag and total drag (including skin-friction drag) and significantly increased lift/drag although maximum heat-transfer rate was increased for the geometries tested.

Introduction

A VARIETY of supersonic and hypersonic vehicles are currently being studied for commercial and military applications. The high-speed civil transport (HSCT) aircraft is designed to cruise at approximately $M_\infty = 2.4$ and seeks to overcome economic and environmental barriers that have limited the success of previous supersonic commercial concepts. Other supersonic flight vehicles of significant interest include single-stage-to-orbit (SSTO) and multistage launch vehicles, tactical and strategic hypersonic and supersonic missiles, hypersonic cruise aircraft, and planetary entry vehicles. These vehicles are similar in that their range, payload mass fractions, and economic feasibility are extremely sensitive to aerodynamic drag.

A discussion of the effects of drag reduction on such supersonic vehicles is given by Bushnell.[1] If the lift/drag (L/D) of the HSCT at cruise is increased by just 10%, there would be a significant impact on the economy and success of that vehicle. Proposed hypersonic vehicles such as the National Aerospace Plane have not advanced because, in part, of diminishing projected payload margins and concerns regarding airbreathing engine capabilities. As pointed out in Ref. 1, drag reductions allow lower fuel requirements and can lead to reduced operating costs and reduced sonic boom and noise effects. Reviews of supersonic drag-reduction techniques and their impact on aircraft performance are given by Bushnell,[1] Hefner and Bushnell,[2] and Jones.[3]

The drag on supersonic vehicles can be classified into three different categories: 1) skin-friction drag, 2) drag caused by lift, and 3) zero-lift bluntness (thickness-wave) drag. Skin-friction drag is caused by fluid viscosity and is a function of the total wetted surface area of the vehicle. Drag cuased by lift consists of induced drag and the component of wave drag, which is a function of the inclination of the vehicle surfaces with respect to the freestream direction at a nonzero lift orientation. Finally, the zero-lift bluntness drag is the wave drag from the vehicle's thickness and bluntness of the leading and trailing edges in a zero-lift orientation. The zero-lift bluntness drag (i.e., thickness-wave drag) increases rapidly with freestream Mach number and can be responsible for well over $\frac{1}{3}$ of the total vehicle drag. The present paper focuses primarily on reduction of the zero-lift bluntness drag as a means of reducing the total drag. A reduction of this component of drag and in the total drag can result in increased vehicle range, increased speed, improved fuel efficiency, increased lift/drag ratio, and enhanced performance.

In the present paper a preliminary investigation of a drag-reduction concept for supersonic airfoils and wings is conducted. A wide range of geometric parameters and supersonic flight conditions are considered so that the aerothermodynamic performance of airfoils employing the present concept are characterized.

Overview of Concept

Linearized supersonic theory indicates that for an airfoil of a given thickness the shape that gives minimum zero-lift bluntness drag is the sharp diamond airfoil. However, very sharp leading edges are not practical for a number of reasons:

1) Very sharp leading edges are difficult (and expensive) to manufacture.

2) Some blunting is required for structural strength.

3) The flow over wings with sharp leading edges is very susceptible to separation even at low angles of attack and flight speeds.

4) The heat transfer to sharp leading edges at high supersonic Mach numbers is severe.

For hypersonic vehicles heat-transfer considerations often dictate the design of the nose and the leading edges. The heat transfer to such vehicles is most severe at stagnation points, which occur on the leading edges and nose of the vehicle. Theoretical and numerical predictions of stagnation-point heating have been developed by Fay and Riddell[4] and are also described by Anderson.[5] Kemp and Riddell[6] developed an accurate semi-empirical relation for stagnation-point heat transfer. Theoretical formulations, experimental data, and semi-empirical formulas all agree in the fact that stagnation-point heat transfer is inversely proportional to the square root of the nose or leading-edge radius, i.e.,

$$a_{\text{stag}} \propto 1/\sqrt{r_n}$$

Vehicles flying hypersonically have blunt leading edges, otherwise heating would melt the sharp (i.e., $r_n = 0$) leading edges. With blunting the simple diamond airfoil would be modified to that illustrated in Fig. 1.

For vehicles that cruise at low supersonic Mach numbers, heat-transfer considerations do not dictate the design of the wing leading edges. At subsonic, off-design conditions, such as takeoff, landing, climb and maneuvering flight, blunted leading edges are desirable so that flow separation is prevented. However, the same blunted wing will experience higher drag at supersonic cruise conditions relative to a wing with a sharp leading edge. Ideally, the airfoils considered for such applications would be significantly blunted during subsonic maneuvering phases of flight but then perform more like sharp leading-edge airfoils at supersonic cruise.

The present concept allows for a hollow channel to be opened at supersonic cruise in the airfoil sections that make up the wings, tails, fins, struts, or other appendages of supersonic and hypersonic vehicles. The channel begins at the leading edge of the airfoil with freestream air flowing passively through the channel. This concept can be applied to any airfoil used on a supersonic vehicle but for simplicity is illustrated on the basic symmetric diamond airfoil as shown in Fig. 2. The channel is designed to decrease the zero-lift

*Associate Professor, School of Aerospace Engineering. Senior Member AIAA.

†Graduate Research Assistant, School of Aerospace Engineering. Student Member AIAA.

‡Graduate Research Assistant, School of Aerospace Engineering. Member AIAA.
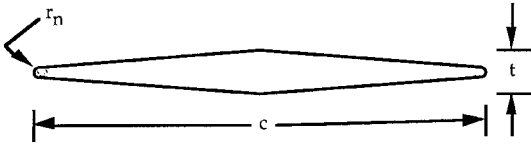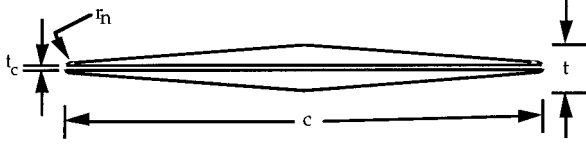
Fig. 1 Schematic of baseline blunted diamond airfoil.
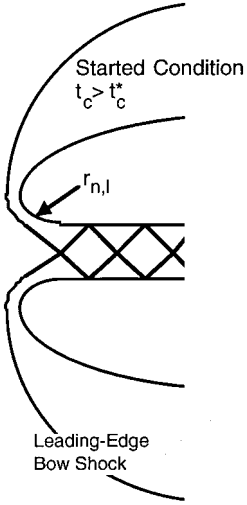

Fig. 2 Schematic of supersonic channel airfoil.

Fig. 3 Schematic of flow-started flow structure possible when channel is used.

Fig. 4 Schematic of flow-choked flow structure possible when channel is used.

bluntness drag relative to an airfoil without a channel (e.g., Fig. 1). For the no-channel airfoil the surface pressure in the stagnation region is high and responsible for much of the drag experienced by the airfoil. However, when the channel concept is used, the vehicle surface that experienced most of the high, near-stagnation pressure is removed. Use of the channel will thus lead to lower wave drag.

When the channel is used, two different leading-edge flow structures are possible. If the channel is sufficiently large, flow will enter the channel supersonically without a normal shock existing in front of the channel (Fig. 3). This is identical to the started condition in supersonic engine inlets and will occur if $t_c > t_c^*$, where t_c^* is the maximum channel thickness for which a choked flow exists. The value of t_c^* depends on the flight Mach number and the airfoil leading-edge radius. When this started condition exists, the heat transfer to the relatively sharp channel lip is much higher than that for the no-channel airfoil.

The second possible flow structure occurs if the channel size is sufficiently small. If $t_c < t_c^*$, then a choked flow condition exists (Fig. 4), a normal shock rests in front of the channel, and the flow enters the channel subsonically. In this case the flow is decelerated significantly through the shock, and the overall flow structure is similar to that of the no-channel airfoil. An effective blunt body is generated by the channel, and the heat-transfer rates at the channel lip are much lower than for the started condition airfoil. One of the objectives of the present study is to quantify the difference in heat-transfer rate between a no-channel geometry and a channel geometry operating in a choked condition. Because low leading-edge heat-transfer rates are required for hypersonic vehicles, the choked flow condition is of greater interest in these applications. Accordingly, most of the analysis considered in the present study is performed for geometries in which $t_c < t_c^*$.

The concept studied in the present paper is somewhat similar to a reverse-flow airfoil in which air is actively pulled into the trailing edge of an airfoil through a duct and ejected forward out of the leading edge of the airfoil.[7] Several studies have been performed
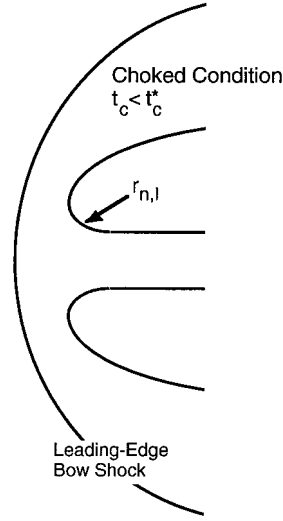
for supersonic flow in which either air or some other gas is forcibly ejected forward out of the blunt nose of axisymmetric bodies.[8-15] This technique causes the existence of a stagnation point in front of the duct and is a means of providing active cooling at the nose. However this technique requires significant power from the engines to eject the gas against a supersonic freestream. In the present study only passive flow of air through the channel is considered.

The present concept is designed to provide an aerodynamic benefit when the leading-edge Mach number is supersonic [i.e., $\beta(s/l) > 1$]. Although wing sweep reduces the Mach number normal to the leading edge, obtaining subsonic leading edges on the main wing, tail surfaces, and fins of hypersonic cruise vehicles requires excessive sweep, and such vehicles are often impractical.[16] For a practical aircraft to achieve nearly global range, its wing leading edges at hypersonic cruise must be supersonic.

The wetted surface area and thus the skin-friction drag will be increased when a channel is utilized. However, if the channel airfoil is designed to operate at a choked condition ($t_c < t_c^*$), then it is possible to maintain a subsonic flow through the channel if the channel wall contours are selected appropriately. In this case the Mach number, velocity, and dynamic pressure inside the channel are significantly lower than the corresponding external supersonic flow quantities. An order-of-magnitude estimate of the ratio of internal friction drag $d_{f_{int}}$ to external friction drag $d_{f_{ext}}$ can be given by

$$\frac{d_{f_{int}}}{d_{f_{ext}}} = \underbrace{\left(\frac{0.5\rho_{int}V_{int}}{0.5\rho_{ext}V_{ext}}\right)}_{\approx 1}\underbrace{\left(\frac{V_{int}}{V_{ext}}\right)}_{\approx \frac{V_{int}}{V_\infty}}\underbrace{\left(\frac{c_{int}}{c_{ext}}\right)}_{\approx 1}\underbrace{\left(\frac{C_{f_{int}}}{C_{f_{ext}}}\right)}_{\approx \frac{Re_{int}^{-\frac{1}{7}}}{Re_{ext}^{-\frac{1}{7}}}}$$

The internal and external mass fluxes are nearly equal, and we assume turbulent flow to relate skin friction and Reynolds number. If we now use Sutherland's law to relate viscosity and temperatures, we get

$$\frac{d_{f_{int}}}{d_{f_{ext}}} \approx \left(\frac{V_{int}}{V_\infty}\right)\left(\frac{\mu_{int}}{\mu_\infty}\right)^{\frac{1}{7}} \approx \left(\frac{V_{int}}{V_\infty}\right)\left(\frac{T_{int}^{\frac{3}{2}}}{T_\infty^{\frac{3}{2}}}\right)^{\frac{1}{7}}$$

Now consider a $M_\infty = 4$ turbulent flow of air around a channel airfoil. The internal channel flow has experienced a $M_\infty = 4$ normal shock, which gives

$$\frac{d_{f_{int}}}{d_{f_{ext}}} \approx \left(\frac{1}{4.57}\right)(1.35) = 0.29$$

Thus, we see that the friction drag on the internal walls can be much less than the friction drag on the external walls if the flow through the channel remains subsonic.

Overall, the channel will yield lower wave drag and increased skin-friction drag. The key questions become the following: For

what airfoil geometries and flight conditions will the decrease in wave drag be more than the increase in skin-friction drag? Is the total drag reduced? The present paper seeks to answer these questions in the next several sections through numerical experiments at selected conditions and then through a systematic consideration of a wide range of flight conditions. This study focuses on the aerothermodynamic performance of generic airfoils and wings employing the channel concept.

Results: Initial Numerical Experiments

Two-Dimensional Airfoil Geometries

The baseline geometry selected for the present drag-reduction analysis is the blunted diamond airfoil (see Fig. 1). Rather than investigate use of the channel on a nearly infinite variety of nonsymmetric, supersonic airfoils considered for various supersonic applications, the generic, diamond airfoil was selected because of its very low drag. In fact, for a given t/c, no airfoil in supersonic flight has lower thickness-wave (i.e., zero-lift bluntness) drag than the sharp diamond airfoil. The present study thus seeks to determine if use of a channel can improve the drag behavior of the blunted diamond airfoil, which inherently experiences low drag. An investigation of the myriad of channel entrance and exit locations on a variety of cambered airfoils remains for future study, and such a study is warranted if the channel shows benefit for generic diamond airfoils.

The baseline, no-channel airfoil selected for most of the analysis is 5% thick with a chord length of 1.0 m. The nose radius is 5 mm, and channel sizes from 2 to 16 mm were evaluated on two-dimensional airfoils. The channel-airfoil geometries are created by carving away a slice about the centerline of the baseline geometry. This creates sharp leading and trailing edges in the channel airfoil. Several channel entrance shapes were tested including those with sharp edges and those with rounded edges at the channel entrance. In addition, airfoils whose channel walls diverge slightly were also tested. Fig. 5 illustrates the various airfoil geometries tested, and the key parameters of the two-dimensional airfoils tested are given in Table 1. The following terminology is used to describe the airfoils: no-channel (baseline) airfoil (NC), sharp-nose straight-channel airfoil (SNSC), round-nose straight-channel airfoil (RNSC), and round-nose diverging-channel airfoil (RNDC).

Analysis Techniques

The flowfields around the geometries considered in this study were predicted using two approaches. Reynolds-averaged Navier–Stokes predictions of aerodynamic and thermal loads on the bodies are obtained using GASP, developed by Aerosoft, Inc. This computer code is a well validated, multizone, finite volume solver. Both laminar simulations and fully turbulent simulations using the Baldwin–Lomax turbulence model were conducted for the present numerical experiments. No attempt to model the exact turbulent transition location was attempted. Consequently, the true performance of the airfoils considered can be expected to be between that of the predicted fully laminar and the fully turbulent results. The third-order-accurate, upwind-biased Roe flux-difference-splitting scheme was utilized, and frozen flow was assumed in each of the simulations. Both the external and internal channel flows are computed simultaneously, in a fully coupled manner, without a backpressure boundary condition specified at the exit of the channel. The two-dimensional computational grids used in the results presented contained approximately 16,000 grid points in each plane. The effects of grid refinement and changes in grid zone topology on the numerical predictions were analyzed in a variety of studies on baseline and channeled airfoils. For example, it was found that with a grid consisting of only one-third the number of grid points (i.e., 5000 points) the drag coefficient is within 1% of the predicted value with 16,000 points per plane. Based on these and similar studies, the estimation is made that the Navier–Stokes lift and drag results presented are within 1% of a solution obtained on a very fine computational grid.

The second approach used to determine aerodynamic loads is based on a classical shock-expansion technique coupled to a semi-empirical, compressible skin-friction drag prediction. This methodology is less accurate than the Navier–Stokes procedure but is of particular value because of its computational efficiency. It is used to efficiently consider use of a channel for a wide range of flight conditions and also provides an independent, back of the envelope comparison of the GASP results. The external airfoil geometries are modeled with eight linear panels. Pressure forces are determined by modeling oblique shocks and Prandtl–Meyer expansions, which begin at the panel junctions. The laminar skin friction on each of the eight panels is approximated using

$$C_f = \frac{0.664\sqrt{C^*}}{\text{Re}_{\Delta_{le}}}$$

where C^* is the Chapman–Rubesin parameter and is based on the reference temperature obtained from Eckert.[17] The Van Driest II method (see Ref. 18), which is valid for a wide range of Reynolds and Mach numbers for attached flat plate boundary layers, is utilized for turbulent skin-friction estimates. The present shock-expansion approximation cannot model the subsonic region behind the leading-edge bow shock and cannot model boundary-layer separation. Despite the approximate nature of the shock-expansion approach, the results are within 15% agreement with the laminar and turbulent Navier–Stokes predictions performed with GASP, and this tool is quite useful for parametric studies.

Two-Dimensional Aerodynamic Performance at Zero Lift

The first series of numerical results are for two-dimensional flow around airfoils with a freestream Mach number of 2.4 and an altitude of 12 km. These calculations can be thought of as modeling the low supersonic flow around unswept fins or wings, or as modeling the flow normal to the leading edge of a hypersonic vehicle with a swept leading edge.

Computed Mach contours for laminar flow around the SNSC-1 airfoil are given in Fig. 6. The main characteristics of a flow including the bow shock at the leading edge caused by bluntness, expansion of the flow as it bends around the top to reach its maximum speed, and subsequent compression at the trailing edge as it turns and slows down to join the freestream are captured well. Separation does not occur at midchord despite the abrupt change in slope at that location for SNSC-1 and the other airfoils described in Table 1. For the SNSC-1 airfoil the flow enters the channel subsonically and remains subsonic through most of the channel. The internal flow slowly accelerates (as the internal boundary-layer grows) and

Table 1   Geometric parameters of two-dimensional airfoils

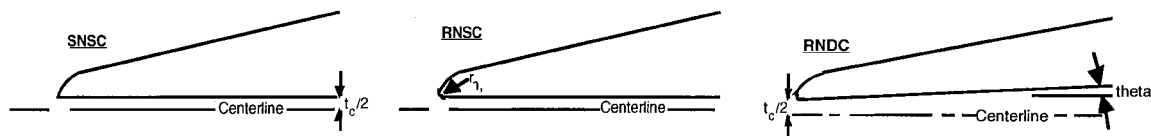| Airfoil	t_c	$r_{n,l}$	θ	t	r_n	c
NC	——	——	——	0.05	0.005	1.0
SNSC-1	0.004	0	0	0.05	0.005	1.0
SNSC-2	0.008	0	0	0.05	0.005	1.0
SNSC-3	0.016	0	0	0.05	0.005	1.0
SNSC-4	0.002	0	0	0.05	0.005	1.0
SNSC-5	0.004	0	0	0.054	0.005	1.0
RNSC	0.004	0.0005	0	0.05	0.005	1.0
RNDC	0.004	0.0005	0.1	0.05	0.005	1.0

Fig. 5   Schematic of channel geometries considered.

becomes supersonic near the end of the channel. Even near the end of the channel, distinct boundary layers and a large inviscid core exist. Thus, the flow in the channel for these conditions does not correspond to fully developed pipe flow.

One of the key questions to be addressed in this study is whether a net decrease in drag occurs through use of a channel. Channel airfoils with several channel thicknesses were investigated, and the drag results are presented in Table 2. We see that when the channel is used, significant drag reductions (including skin friction) from 33 to 78% are achieved and the magnitude of drag reduction increases with channel size. However, of the three channel sizes investigated for these flight conditions, only the case with $t_c =0.004$ m (i.e., SNSC-1) exhibits a choked-channel entrance with a normal shock in front of the leading edge. With larger channel sizes the started condition is observed, and the flow enters the channel supersonically. Although the large channel geometries (e.g., SNSC-2 and SNSC-3) exhibit very low drag, they experience much higher heat-transfer rates at the channel entrance. For the remainder of the cases considered, results are only presented for airfoils with channel sizes small enough to have a choked entrance, and heat-transfer results are further discussed in a later section of this paper.

Channel geometries in which the channel entrance was rounded and those in which the channel walls diverge slightly were also investigated. A comparison of the inviscid/viscous drag breakdown for the NC and various channel-airfoils (SNSC-1, RNSC, RNDC) is shown in Fig. 7 for laminar flow. We see that each of the channel airfoils experiences approximately 35% lower total drag relative to the no-channel geometry at a zero-lift condition. We see that the decrease in wave (inviscid) drag more than makes up for the increase in skin-friction (viscous) drag. The diverging-channel geometry experiences somewhat lower drag than the straight-channel airfoils. When a diverging channel is used, the pressure on the internal channel walls creates a force component which acts in the upstream direction, thereby further lowering drag. However, although the internal channel flow enters subsonically it becomes supersonic just after the channel entrance. Conversely, in the straight-channel cases the flow remained subsonic through most of the channel. The higher dynamic pressure in the diverging-channel geometry causes this airfoil to experience higher viscous drag than the straight-channel airfoils.

These Navier–Stokes simulations were repeated assuming fully turbulent flow (Baldwin–Lomax model) on the external and internal walls. The drag breakdown for the turbulent simulations is given in Fig. 8. Although in turbulent flow skin friction is a larger component

of the total drag, the channel airfoils experience from 14 to 21% total drag relative to the no-channel geometry.

We now consider whether the drag reductions demonstrated in the preceding results exist at other flight conditions. A parametric study of a wide range of Mach numbers and altitudes was conducted using the viscous shock-expansion procedure. Figures 9 and 10 show the results of analysis of the NC and the SNSC-1 airfoils for laminar and fully turbulent flow, respectively. Mach numbers from 1.3 to 2.5 and flight altitudes from sea level to 50 km were investigated to determine the range of drag reduction afforded by the channel concept. At $M_\infty =2.5$ a drag reduction of over 30% is observed at low altitudes for laminar flow and over 20% for turbulent flow. These results agree with the Navier–Stokes predictions already presented. In a sense the SNSC-1 airfoil is designed for $M_\infty =2.5$ because it has the largest channel size, which yields a choked flow at the channel entrance for $r_n =0.005$ m. At off-design conditions (i.e., $M_\infty < 2.5$)
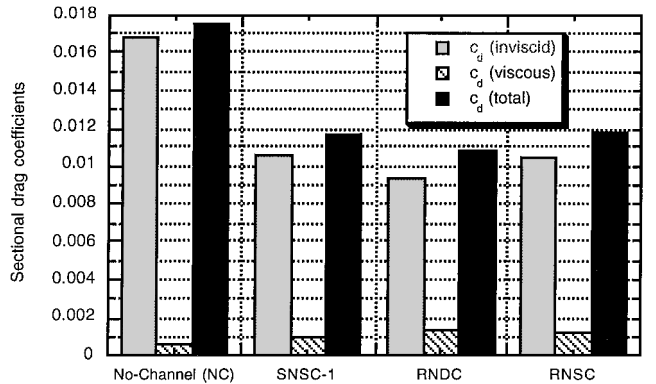
Fig. 7 Computed drag breakdown for no-channel and channel airfoils in laminar flow: $M_\infty = 2.4$, $\alpha = 0$ deg, and $h = 12$ km.
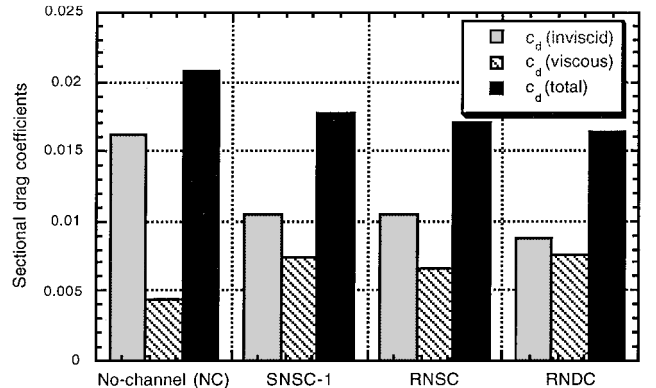
Fig. 8 Computed drag breakdown for no-channel and channel airfoils in fully turbulent flow: $M_\infty = 2.4$, $\alpha = 0$ deg, and $h = 12$ km.

Table 2 Drag results computed with GASP
($M_\infty = 2.4$, $\alpha = 0$ deg, 12 km)

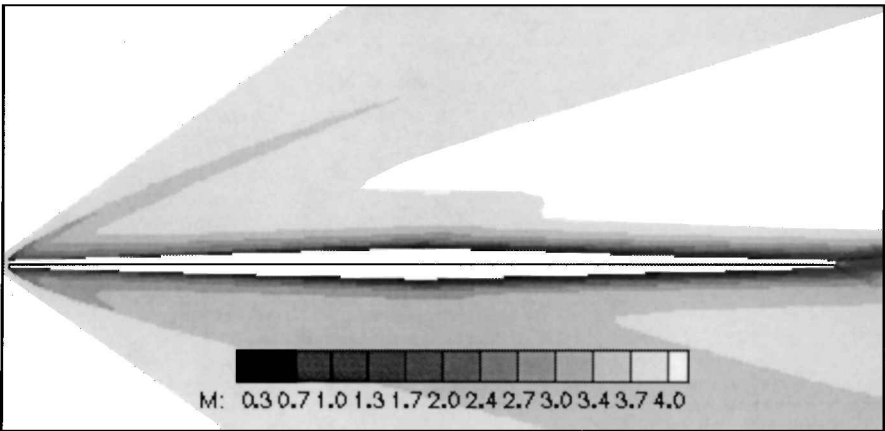| Airfoil	t_c	c_d	c_d decrease, %
NC	——	0.01748	——
SNSC-1	0.004	0.01168	33
SNSC-2	0.008	0.00614	65
SNSC-3	0.016	0.00378	78

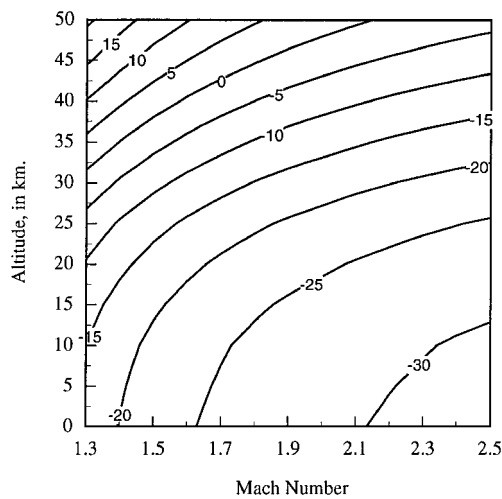**Fig. 6 Computed Mach contours for SNSC-1 airfoil:** $M_\infty = 2.4$, $\alpha = 0$ deg, and $h = 12$ km.

Fig. 9 Predicted percentage change in drag caused by channel for 5% thick blunted diamond airfoil designed for choked flow at M_∞ = 2.5. Laminar flow assumed.
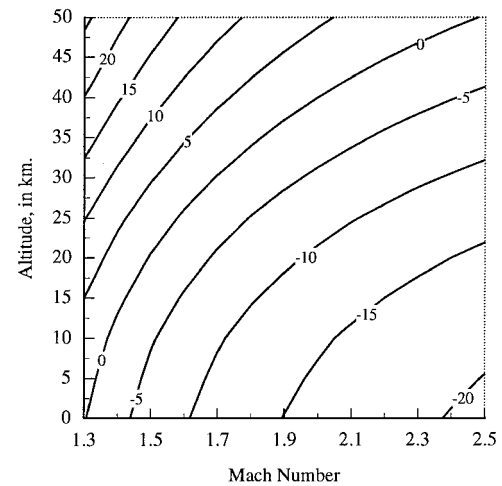

Fig. 10 Predicted percentage change in drag caused by channel for 5% thick blunted diamond airfoil designed for choked flow at M_∞ = 2.5. Fully turbulent flow assumed.

Table 3 Drag results comparing no-channel and channel airfoils with the same enclosed area (M_∞ = 2.4, α = 0 deg, 12 km)

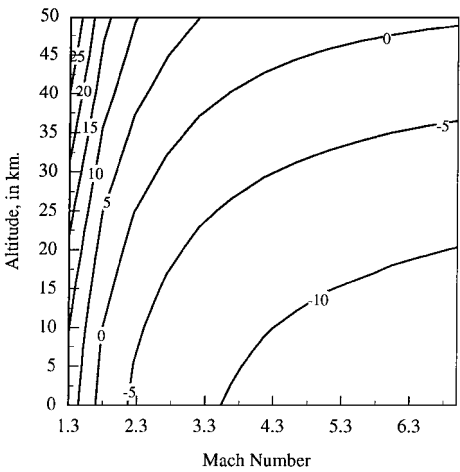| Airfoil	t_c, m	t, m	c, m	Enclosed area, m^2	c_d	c_d decrease
NC	——	0.05	1.0	0.05	0.018	——
SNSC-5	0.004	0.054	1.0	0.05	0.013	28%

Fig. 11 Predicted percentage change in drag caused by channel for 5% thick blunted diamond airfoil designed for choked flow at M_∞ = 7. Fully turbulent flow assumed.

main wing enclosed volume is also used for fuel storage. Thus it is also useful to compare the baseline airfoil with the SNSC-5 airfoil, which has the same enclosed area. The results of a viscous shock-expansion comparison of such airfoils is given in Table 3. Although the SNSC-5 airfoil is somewhat thicker than the baseline no-channel airfoil, it has 28% less drag. Thus, even if no loss in wing volume can be tolerated, the channel airfoil gives significantly improved performance.

Two-Dimensional Aerodynamic Performance at Lifting Conditions

The results of the preceding subsections showed that use of a channel can reduce drag at zero lift. In this section the flow structure and the drag at lifting conditions are compared for no-channel and channel-airfoil geometries.

Figure 12 shows pressure contours computed using GASP for the NC, SNSC-1, RNSC, and RNDC airfoils at α = 5 deg. The choking of the flow for the channel cases at angle of attack is clearly visible, and the overall flow structure that was observed at α = 0 deg is maintained. However at angle of attack the flow at the channel entrance is nonsymmetric. A suction peak occurs above the lower channel wall, and a compression occurs at the upper channel wall. The flow through the channel becomes nearly symmetric shortly downstream of the entrance region.

Computed sectional drag coefficients (from Navier–Stokes simulations) are shown as a function of angle of attack in Figs. 13 and 14 for laminar and fully turbulent flow respectively. We see that the channel airfoils experience lower total drag than the no-channel airfoil for all angles of attack tested. Use of the channel results in a nearly uniform downward shift in sectional drag coefficient. For laminar flow the RNDC experiences slightly lower drag than the straight-channel cases.

The lift generated by the airfoils is virtually unaffected by use of the channel geometries considered. The drag reduction experienced at all angles of attack thus allows significant net increases in aerodynamic efficiency, i.e., L/D. L/D vs angle of attack is shown in Fig. 15 for laminar flow. The maximum L/D is increased by approximately 35% for laminar flow and approximately 20% for fully turbulent flow when the channel is used. The results of these angle-of-attack studies and the previous parametric studies indicate that improved performance can be achieved at variable and off-design flight conditions. There is no abrupt change in sectional drag or lift at any angle of attack or supersonic Mach number.

a smaller but significant drag reduction is seen. For Mach numbers larger than the design Mach number (i.e., M_∞ > 2.5), the SNSC-1 airfoil will swallow the leading-edge shock, and the drag reductions will be even greater; however, heat-transfer rates will increase. From Figs. 9 and 10 we see that, as altitude is increased, with M_∞ held constant, the drag reduction afforded by the channel decreases. This is a consequence of the fact that as altitude increases the Reynolds number decreases and the component of drag caused by skin friction increases. Although the channel increases the component of drag caused by skin friction, we see that at M_∞ = 2.5 the channel results in a net reduction in total drag from sea level up to an altitude of 50 km.

A similar analysis was performed for the SNSC-4 airfoil, which is designed to provide a choked flow for M_∞ < 7.0. The result of this analysis is shown in Fig. 11. We see that at sea level the channel reduces the drag by over 10% relative to the baseline no-channel airfoil. The channel provides drag reduction for a wide range of Mach numbers and altitudes from sea level to over 45 km.

The SNSC airfoils whose results have been described were designed by simply carving out a channel from a no-channel airfoil. Thus whereas the airfoil thickness (i.e., distance from the top to the bottom of the airfoil) is the same for each of the airfoils, the total airfoil enclosed area is somewhat different for each case. For the SNSC-1 airfoil (t_c = 0.004 m) the enclosed area loss is small (8%) while the zero-lift drag reduction is large (33% for SNSC). However, the area inside an airfoil, or actually the volume in the wing, is important because it is needed for structural members. Often the

a) NC baseline airfoil: $C_d = 0.03297$

c) RNSC airfoil: C_d reduction = 22%

b) SNSC-1 airfoil: C_d reduction = 22%
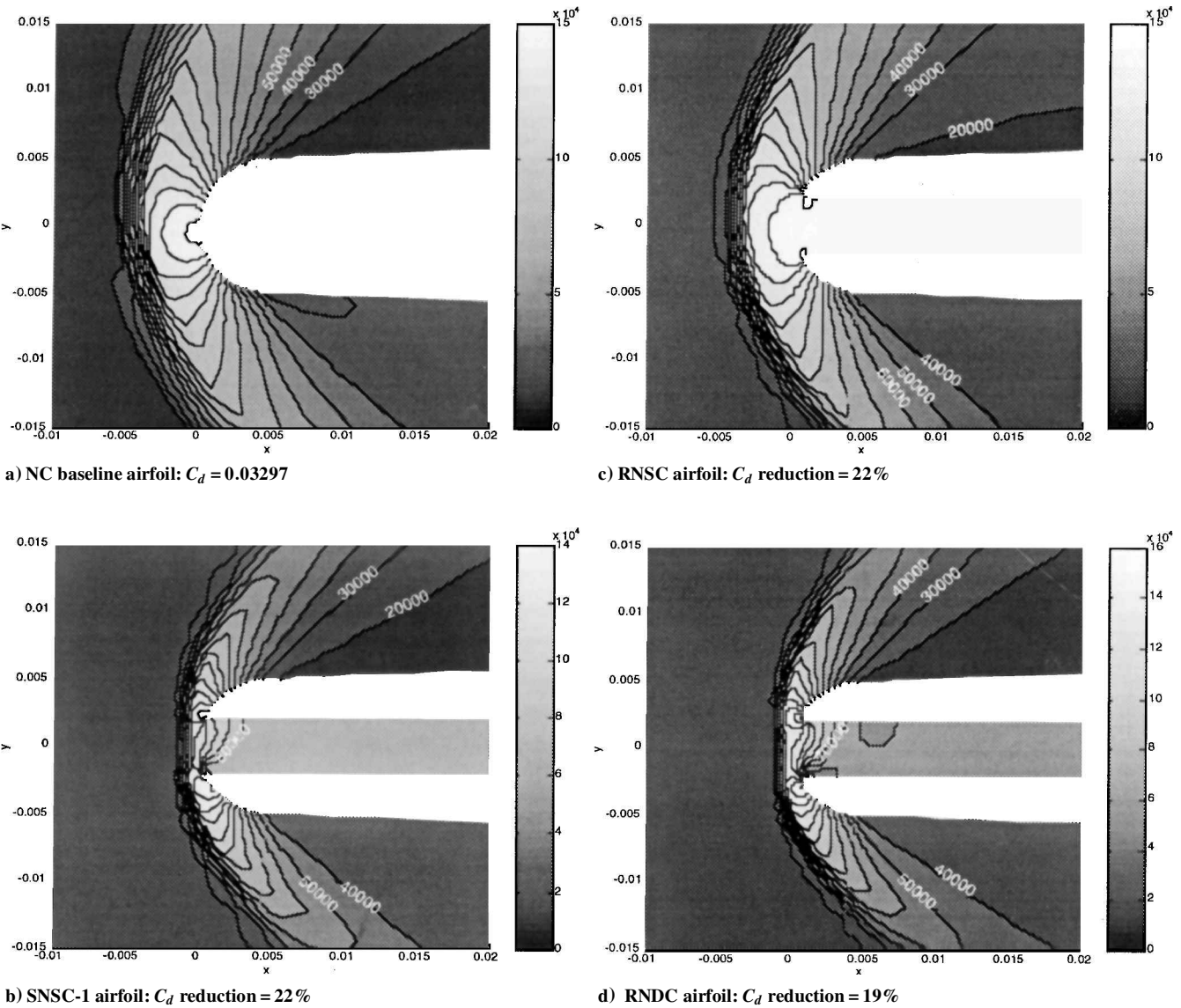
d) RNDC airfoil: C_d reduction = 19%

Fig. 12   Computed static pressure contours near leading edge at $\alpha = 5$ deg, $M_\infty = 2.4$, and $h = 12$ km.
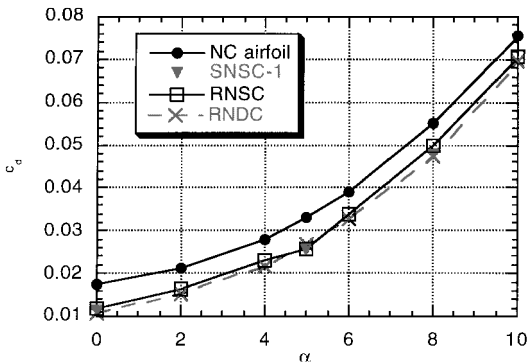

Fig. 13   Sectional drag coefficient vs angle of attack for no-channel and channel airfoils in laminar flow: $M_\infty = 2.4$ and $h = 12$ km.
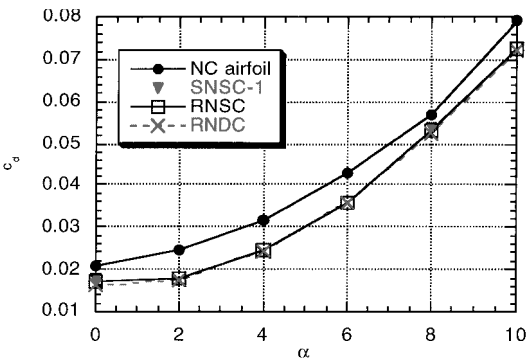
Fig. 14   Sectional drag coefficient vs angle of attack for no-channel and channel airfoils in fully turbulent flow: $M_\infty = 2.4$ and $h = 12$ km.

Heat-Transfer Results

Heat-transfer rates were predicted using the Navier–Stokes solver by specifying a constant wall temperature of 300 K and analyzing $M_\infty = 2.4$ flow around the airfoils at $\alpha = 0$ deg. The heat-transfer rates near the leading edges of the NC and the RNSC are shown in Fig. 16. The heat-transfer predictions are found to be significantly more sensitive than lift and drag predictions to computational grid refinement and topology changes. Based on these grid studies, it is estimated that the heat-transfer results in Fig. 16 are within 15% of the predictions on a very fine computational grid.

Figure 16 shows that the maximum heat-transfer rate for the channel-airfoil geometry selected is higher than that for a baseline no-channel airfoil. For the test conditions selected, the RNSC has a choked-channel entrance, and its maximum heat-transfer rate is lower than for the started condition case (not shown). Although the effective blunt-body flow structure generated by the choked-channel reduces the heat transfer relative to a started-condition geometry, the channel airfoil experiences a higher maximum heat-transfer rate than the conventional no-channel airfoil in the present preliminary study. When a channel is used, the maximum heating occurs at
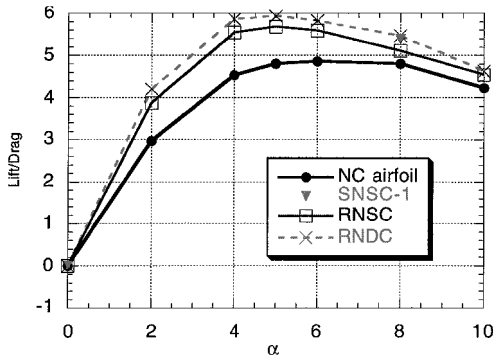
Fig. 15   L/D vs angle of attack for no-channel and channel airfoils in laminar flow: $M_\infty = 2.4$ and $h = 12$ km.
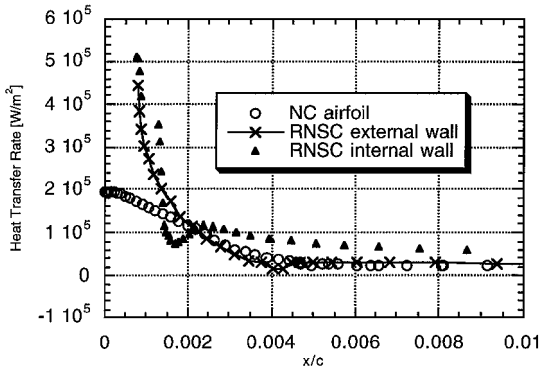

Fig. 16   Computed heat-transfer rate near the leading edge for no-channel and RNSC airfoils in laminar flow: x/c is streamwise distance/chord, $M_\infty = 2.4$, $\alpha = 0$ deg, and $h = 12$ km.

the channel lip, and additional studies have been conducted, which indicate that this heating rate decreases substantially as $r_{n,l}$ is increased. Gupta and Ruffin demonstrated that the maximum heat-transfer rate using a channel with a sufficiently rounded leading edge can produce heat-transfer rates that are not higher than geometries without a channel.[19] Future studies of the channel concept should seek to quantify the variation of maximum heat transfer with $r_{n,l}$ and maximize the improvement in aerodynamic performance without causing a penalty in maximum heat-transfer rate.

Conclusions

A proof-of-concept study is performed for a supersonic channel-airfoil concept, which can be applied to the leading edges of wings, tails, fins, struts, and other appendages of aircraft, atmospheric entry vehicles, and missiles in supersonic flight. It is designed to be beneficial at conditions in which the leading edge is significantly blunted and the Mach number normal to the leading edge is supersonic.

With a sufficiently small channel a normal shock exists in front of the leading edge thus creating a choked entrance condition. The normal shock decelerates the channel entrance flow and reduces gradients around the channel lip relative to a started condition geometry. However, even when a choked entrance condition exists, the maximum heat-transfer rate on a channel-airfoil geometry can be significantly greater than that for a no-channel airfoil. Additional study of channel airfoils is needed to determine if use of an appropriate channel lip radius can eliminate this increase in heat transfer while still yielding significantly reduced drag.

The supersonic channel-airfoil concept is found to reduce total drag and increase L/D by over 30% for laminar flow and over 20% for turbulent flow relative to geometries without channels. Future studies should investigate the possibility of enhancing airfoil lift by using channels that do not lie symmetrically along the airfoil centerline.

The ability of the channel concept to significantly improve the aerodynamic performance of blunted vehicles in supersonic flight makes it potentially beneficial for several types of applications.

These applications include blunted planetary entry vehicles and supersonic cruise aircraft.

Planetary entry vehicles are significantly blunted so that heating rates will be tolerable during the initial phases of atmospheric insertion. Although high drag is desirable for the initial phases of these missions, it would be beneficial to have the ability to open a channel after the maximum heating-rate flight condition has been passed. Doing so would substantially increase the L/D, and high L/D is required for entry vehicles to achieve the cross-range capability necessary for precise selection of landing or impact site. Supersonic cruise aircraft whose leading edges are blunted for low-speed-stall mitigation can benefit from a channel that opens along at least part of the wing span at supersonic cruise.

References

[1]Bushnell, D., "Supersonic Aircraft Drag Reduction," AIAA Paper 90-1596, June 1990.

[2]Hefner, J. N., and Bushnell, D. M., "An Overview of Concepts for Aircraft Drag Reduction," *Special Course on Concepts for Drag Reduction*, AGARD Rept. 654, von Kármán Inst., Rhode-St-Genese, Belgium, 1977, pp. 1-1-1-30.

[3]Jones, R. T., "Aerodynamic Design for Supersonic Speeds," *Advances in Aeronautical Sciences*, Vol. 1, No. 1, 1959, pp. 34–52.

[4]Fay, J., and Riddell, F., "Theory of Stagnation Point Heat Transfer in Dissociated Air," *Journal of Aeronautical Sciences*, Vol. 25, No. 2, 1958, pp. 73–85.

[5]Anderson, J. D., *Hypersonic and High Temperature Gas Dynamics*, McGraw–Hill, New York, 1989, pp. 250–300.

[6]Kemp, N., and Riddell, F., "Heat Transfer to Satellite Vehicles Re-Entering the Atmosphere," *Jet Propulsion*, Vol. 27, No. 2, 1957, pp. 132–137.

[7]Kuchemann, D., "Some Aerodynamic Properties of a New Type of Aerofoil with Reversed Flow Through an Internal Duct," Royal Aircraft Establishment, TN Aero 2297, Farnborough, England, U.K., 1954.

[8]Sutton, E. P., and Finley, P. J., "The Flow of a Jet from the Nose of an Axisymmetric Body in a Supersonic Airstream," *Archiwum Mechanika Stosowanej*, Vol. 3, 1964, p. 781.

[9]Finley, P. J., "A Preliminary Investigation of the Steadiness of a Free Stagnation Point," *Journal of the Department of Engineering, University of Malaya*, Vol. 4, No. 1, 1965, p. 8.

[10]Finley, P. J., "The Flow of a Jet from a Body Opposing a Supersonic Free Stream," *Journal of Fluid Mechanics*, Vol. 26, Pt. 2, 1966, pp. 337–370.

[11]McMahon, H. M., "An Experimental Study of the Effect of Mass Injection at the Stagnation Point of a Blunt Body," California Inst. of Technology, GALCIT Hypersonic Research Project Memo 42, Pasadena, CA, 1958.

[12]Lam, S. H., "Interaction of a Two Dimensional Inviscid Incompressible Jet Facing a Hypersonic Stream," U.S. Air Force Office of Scientific Research, TN 59-274, Rept. 447, March 1959.

[13]Eminton, E., "Orifice Shapes for Ejecting Gas at the Nose of a Body in Two Dimensional Flow," Royal Aircraft Establishment, TN Aero 2711, Farnborough, England, U.K., Aug. 1960.

[14]Warren, C. H. E., "An Experimental Investigation of the Effect of Ejecting a Coolant Gas at the Nose of a Blunt Body," *Journal of Fluid Mechanics*, Vol. 8, Pt. 3, 1960, pp. 400–417.

[15]Reid, J., and Tucker, L. M., "Forward Ejection from Swept and Unswept Leading Edges," Royal Aircraft Establishment, TR 68095, Farnborough, England, U.K., 1968.

[16]Kuchemann, D., *The Aerodynamic Design of Aircraft*, Pergamon, Oxford, 1978, pp. 228, 493.

[17]Eckert, E. R. G., "Engineering Relations for Friction and Heat Transfer to Surfaces in High Velocity Flow," *Journal of Aeronautical Sciences*, Vol. 22, 1955, pp. 585–587.

[18]Hopkins, E. J., "Charts for Predicting Turbulent Skin Friction from the Van Driest Method (II)," NASA TN D-6945, Oct. 1972.

[19]Gupta, A., and Ruffin, S. M., "Aerothermodynamic Design of Supersonic Channel-Airfoils for Drag Reduction," AIAA Paper 97-5572, Oct. 1997.

J. C. Hermanson
Associate Editor